Senior Thesis

Laboratory Analysis of Vesicle Size Distribution in Basaltic Lava Flows: Application to Atmospheric Pressure Measurement

By:

Joseph Maus
1993

Submitted as partial fulfillment of the requirements for the degree of Bachelor of Science in the Geological Sciences at the Ohio State University.

Approved by:

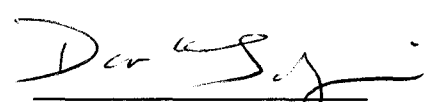

Dr. Dork Sahagian

Introduction.

Why study vesicle (bubble) size distribution in lava flows? There are many reasons. With regards to this research, the vesicularity near the top of the flow is related to that near the base of the flow. These vesicularities are normalized by initial average bubble size and, after normalization, the vesicularities can be used as a rather sensitive barometer of atmospheric pressure at the time of flow emplacement using a simple relation. Other reasons include:

- The mechanism of ascent and eruption of magma may be reflected in the initial size distribution of the vesicles.
- In solidifying bodies of magma, distribution of vesicles may reveal the mechanism(s) involved in the de-gassing of the magma.
- Tops and bottoms of beds can be inferred in structurally complex areas by using vesicular zones characteristic of flow tops.
- Flow emplacement processes and rates may be observed in the final distribution of vesicles. (Sahagian, 1985)

The vesicular nature of basaltic lava flows allows for the determination of ancient elevations and/or sea-level atmospheric pressure at time of emplacement. This is possible because the total pressure in a bubble is the sum of the hydrostatic pressure of lava overburden and ambient atmospheric pressure. Gas bubbles exsolve from magma during their rise to the surface (Sparks, 1978). Gas exsolved during basaltic eruptions is predominately H_2O and it is thought these (water vapor) bubbles form at $\leq$120 meters depth below the surface (Gerlach, 1986; Mangan et al, 1993). The sizes of these bubbles can be characterized by a distribution around a mean, and they change as they rise within the flow after emplacement, but before solidification. Final size distribution is also changed by the coalescence of smaller bubbles into larger bubbles. Bubbles rise and coalesce

within a fluid interior sandwiched between fronts of solidification that advance inward with time from both the top and bottom of the fluid simultaneously (Sahagian et al, 1989). As the solidus fronts migrate inward, bubbles are trapped and frozen in place. No further movement or growth is possible.

A numerical model has been developed (Sahagian, 1985) which predicts the effects of rise and coalescence of bubbles within the melt. This model provides the basis for understanding the relation between initial (eruptive) bubble size distribution, and final (observed) bubble size distribution. The model calculates a basalt flow of given thickness with a constant viscosity (2×10^4p), and a given volume percentage of ideal (spherical) gas bubbles (Sahagian et al, 1989). It is assumed that the spatial distribution of the bubbles throughout the flow are uniform as it is emplaced, since many basaltic magmas are well mixed by convection as they reside in the magma chamber. It may be reasonable to assume convection counters the bubbles tendency to rise (Sahagian et al, 1989; Sahagian, 1985; Spera et al, 1982).

Bubbles of different size rise at different velocities. Final (observed) vesicularity and vesicle (bubble) size distribution are sensitive to the ambient atmospheric pressure. As the bubbles rise through the flow, they expand (decompress) as the hydrostatic pressure of the magma (relative to the bubble's position as it rises through the flow) is reduced. The magma's hydrostatic pressure, in addition to itself, also carries the imprint of the ambient atmospheric pressure. Therefore, the relationship between the vesicular zones in the upper and lower parts of the flow rely "not only on bubble rise and coalescence, but also on flow thickness and atmospheric pressure" (Sahagian et al, 1989). Two bubbles with equal mass, (for example, one at the top of the flow and the other at the bottom) will be subject to different–total pressures due to the difference of the sum of the hydrostatic pressure of the magma and ambient atmospheric pressure on them. Hence, the difference in pressure results in two different volumes for the

bubbles (Sahagian, unpublished manuscript).

One might visualize bubbles of gas rising in a glass of beer as an analogy to our process. But this is not the case. Hydrostatic pressure is essentially constant for the typical glass of beer. A column of beer 30 foot high would be required to increase pressure to 2 bars at the base. Hence, decompressive expansion is not a valid mechanism for bubble expansion in beer. The bubbles increase in volume by sweeping out of the beer dissolved CO_2 as the bubbles rise to the surface (Shafer and Zare, 1991).

Conversely, a typical lava flow will have a pressure gradient in place. Flows only 10 meters thick will have at least 3 bars of pressure at the base of the flow. Hence, bubbles expand as they rise through the pressure gradient, in addition to, growth resulting from coalescence (Mangan et al, 1993; Sahagian et al, 1989).

The objective of the laboratory analysis was to obtain the final (observed) size distribution of these bubbles from natural basalt samples that were collected from the summit and base of Mauna Loa, Hawaii. The vesicles in the basalts were impregnated with plastic, which upon dissolution of the basalt, yielded casts of the vesicles, or "bubbles." The bubbles were counted according to a size regime so vesicularity could be determined from the natural samples. In addition, the altitude, and thus barometric pressure at the time of emplacement of these recent flows, is known. This empirical data provides a rigorous test of the numerical model.

Criteria and Location of Sample Collection.

The samples were obtained from high and low elevations on Mauna Loa on the island of Hawaii. Mauna Loa was chosen for the following reasons: its recent activity, its flows are generally of uniform chemistry and morphology, and its continuity between sea level and its summit, which is greater than 13,000 feet. Only complete flows from base to top were sampled, and then, only if fully

exposed. Three to five samples were obtained from each flow at various locations within the flow. All samples were numbered according to their respective position within the flow (Sahagian, unpublished manuscript). The locations and sample positions of the basalt flows used in this study are given in table 1 and figure 1 (Sahagian, field notes).

Table 1. Sample locations.

Site	Quad name	Elevation, in feet	Flow thickness, in inches	Sample number	Location of sample within flow.
1	Hilo	150	60	1	Top, but a little below inferred pahoehoe surface.
				2	12 down from cliff, 18" down from inferred top.
				3	37" down from inferred top.
				4	Base, 54" or 60" down from inferred top.
2	Piihonua	860	30	5	Top of flow.
				6	Top of sample 6 is 10" below flow top.
				7	Base, three small samples.
3	Piihonua	1100	70	8	Top of cliff, 2" below pahoehoe top.
				9	34" below pahoehoe top.
				10	Base of flow.
				11	Pahoehoe top of flow.
4	Hilo	680	46	12	Just below inferred pahoehoe top, 9" below actual top.
				13	Base of flow.
5	Mauna Loa	13050	40	14	Top of flow.
				15	Base of flow (2 pieces fit together).
6	Mauna Loa	13050	48	16	Top of flow.
				17	Top of sample 31" above base of flow.
				18	Base of flow.
7	Mauna Loa	12900	65	19	Top of flow.
				20	Top of sample is 47" from base of flow.
				21	Top of sample is 34" from base of flow.
				22	Base of flow.
8	Mauna Loa	12900	50	23	Top of flow.
				24	Top of sample is 38" from base.
				25	Base of flow.
9	Mauna Loa	13030	66	26a	Top of flow.
				26b	Top of flow, both a and b, but they do not fit together.
				27	Top of sample is 2" below top of flow.
				28	Top of sample is 42" above base of flow.
				29	Base of flow.

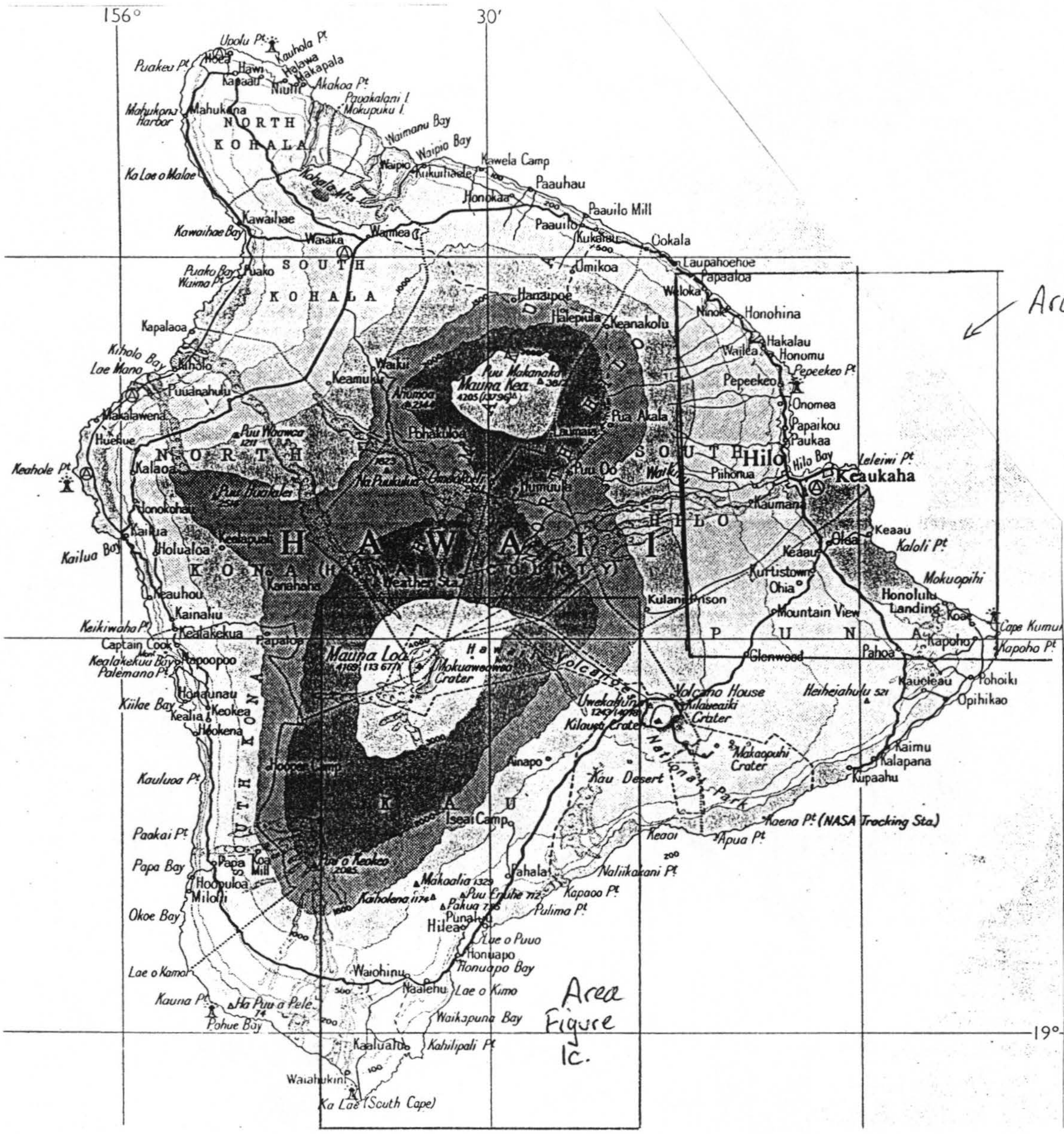

Figure 1a. Location of figures 1b and 1c in relation to the island of Hawaii proper. (The Times atlas of the world, 1985, Hawaii, 1:1,000,000 series, plate 114.

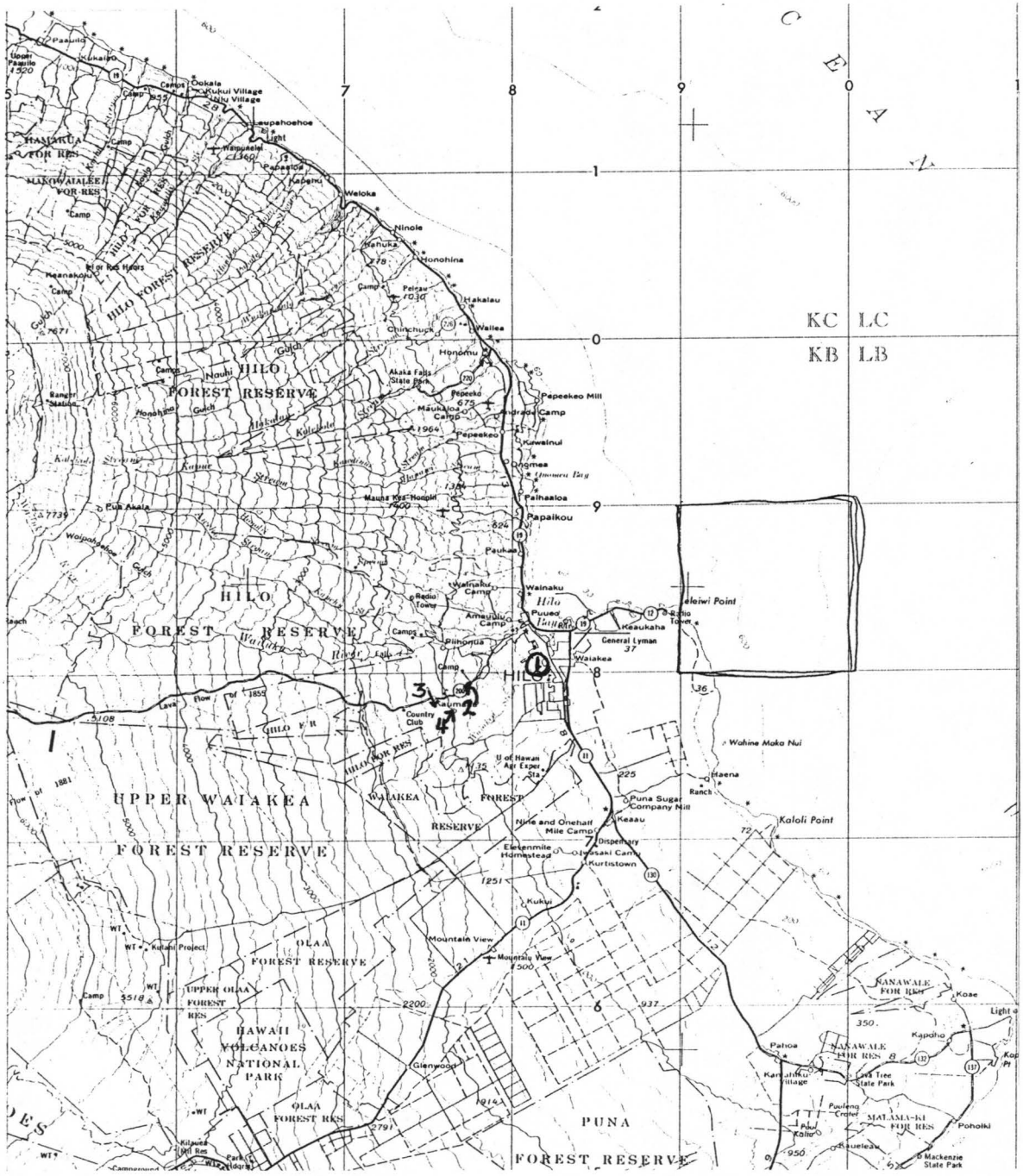

Figure 1b. Location of sample sites 1-4. (USGS base map, 1975, Hawaii, 1:250,000 series)

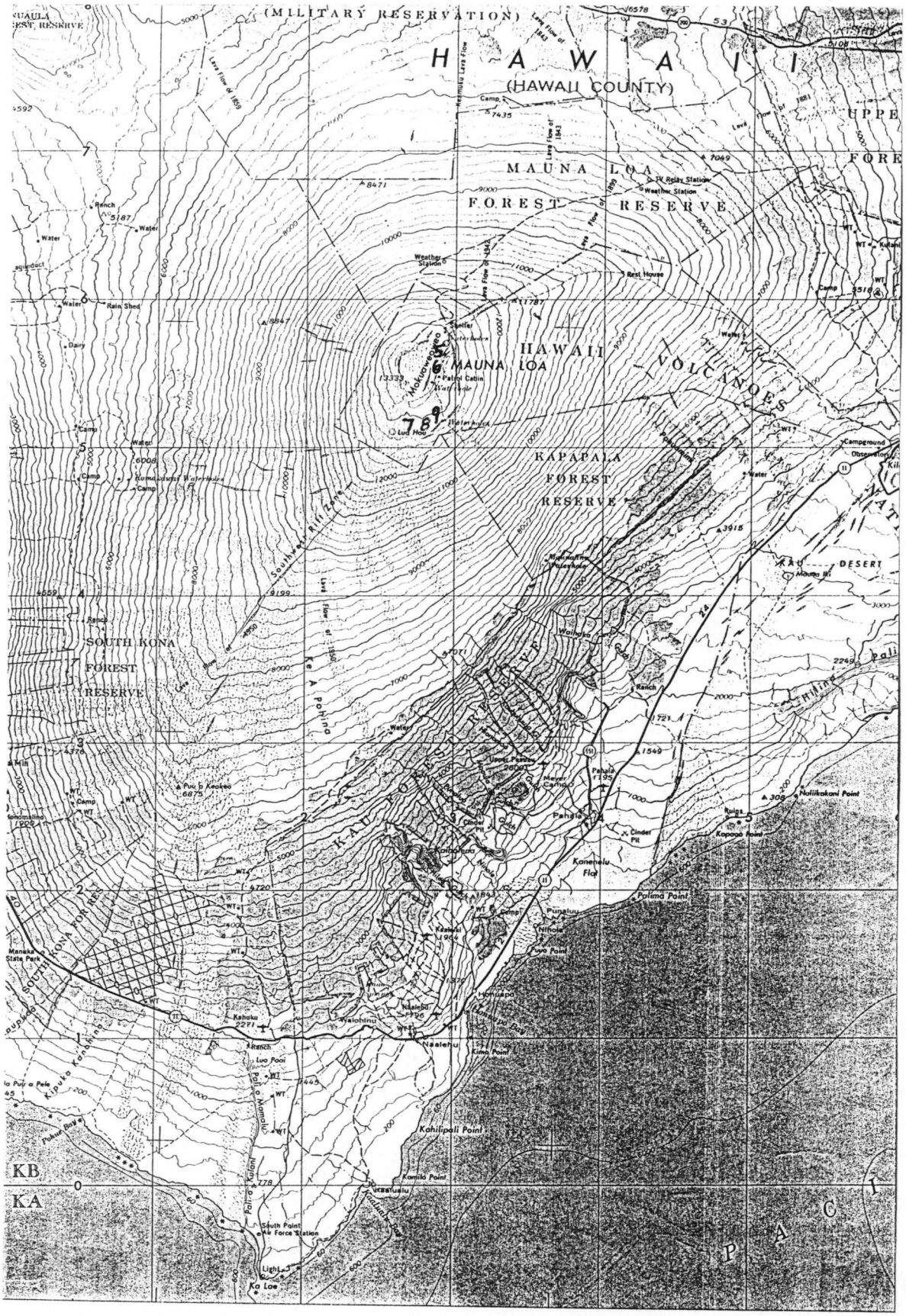

Figure 1c. Location of sample sites 5-9. (USGS base map, 1975, Hawaii, 1:250,000 series)

Laboratory Procedure Overview.

Empirical data gathering of the vesicle (bubble) size distribution of the basalts involved a number of steps. Some steps were modified during the course of the experiment in an attempt to find more accurate ways to obtain the required data. The procedures to obtain vesicle casts from hand samples were as follows:

1) Each hand sample was cut on a rock saw to approximately 5cm long and 3cm on each edge. It was cleaned of cutting material and dried in an oven to remove moisture. The sample was weighed in air and in water to determine density of the rock sample from which bulk vesicularity was calculated. The sample was placed on a platform adjacent to a beaker containing a polystyrene monomer in a bell jar. The bell jar was evacuated by vacuum pump and the sample was caused to fall into the polystyrene monomer. Allowing air to leak slowly into the bell jar had the effect of pumping the monomer into the basalt, to make casts of the vesicles. The sample was cured and trimmed of excess plastic. Afterwards, the sample was immersed in 48% hydrofluoric acid (HF) to dissolve the basalt. After the basalt had dissolved, the solution was neutralized by an aqueous solution of slaked lime (CaOH). The resultant casts were cleaned and separated from the solution by means of sieving. These casts were dried and subsequently counted by size on 1mm graph paper. These procedures were similar to those of Sahagian et al (1989), but included several important refinements.

Laboratory Procedure.

1. Determination of Bulk Vesicularity.

The first task was to determine the bulk vesicularity of the sample. This was done to help establish a relationship between top and bottoms of flows. Two methods were employed.

A. The first method included the following steps: a hand sample was

weighed in air on a triple beam balance. The sample was placed within a plastic bag, and excess air removed by suction. Then, the sample was weighed in water by a modified triple beam balance. The balance was modified to obtain a zero weight indication with the weighing pan immersed in water. For some samples, this method proved to be unreliable. Sharp protrusions, characteristic of basalts, routinely punctured the bag and caused erroneous results. Further, some samples were too small, or too vesicular. In these cases, the bag containing the sample floated on the water, thereby making results unobtainable. It was these shortcomings that led to the development of the second method, employed about half-way through the experiment.

B. The second method involved encasing the samples in paraffin. This method was somewhat more involved, but considerably more reliable.

The first step of this method was similar to the that of the first method, but instead of weight being used to determine bulk vesicularity, water displacement was used. A 500ml graduated cylinder was modified to fit inside a bell jar. The cylinder was filled with water to various levels and the hand samples were cut to fit inside the cylinder. Samples were placed in the cylinder which was inside the bell jar. The bell jar was evacuated and a constant vacuum was maintained for five minutes. This resulted in the near complete loss of air from within the sample's vesicles. (Although air bubbles were observed throughout the entire 5 minutes, their frequency in the last minute was probably trivial.) The bell jar was allowed to return to 1 bar, causing the vesicles to be filled with water. The volume measurement of the displaced water thus represents the volume of the rock alone. The volume measurements could be accurately measured to within ±0.5ml. This value was then recorded (see Appendix A).

Next, the hand samples were placed in an oven at 80°C for a minimum of 24 hours, followed by a cooling down period of at least an equal time. Secondly, the samples were wrapped tightly with a single layer of masking tape and were

marked with a sample number. Further, a wire twist-tie was secured to the sample in preparation for the following step.

The third step of this process involved the dipping of the samples in melted paraffin. This dipping was repeated for each sample 3 times to insure the sample would be sealed. After sealing and cooling, the wire twist-tie was cut as close to the sample as possible.

Finally, the sample was again placed in a known volume of water and its total displacement was measured. Again, accuracy could be reasonably assured to within ±0.5ml. This value was recorded (see appendix A).

After the sample's encased volume was determined, the wax and masking tape cover were carefully removed from the sample. This encasement material was weighed on a triple-beam balance. The masking tape and paraffin density were determined by weighing a quantity of masking tape and paraffin and determining their respective volume displacements in a 10ml graduated cylinder filled with a known quantity of water. The precision of these density measurements is within ±0.01g/ml. These values were recorded (see appendix A).

Bulk vesicularity was then computed for all samples, using both methods, by the following formula:

$$\text{BulkVesicularity} = \frac{((W_{de} - 100) - (W_{em}/\rho_{em})) - W_{di}}{((W_{de} - 100) - (W_{em}/\rho_{em}))} \qquad (1)$$

Where W_{te} is the water displacement of the encased sample (in ml), W_{em} is the weight of the encasement materials (in grams), ρ_{em} is the density of the encasement materials (in g/ml), and W_{di} is the water displacement with the sample impregnated with water (in ml). The results of these calculations are also

given in appendix A at the end of this report.

A Better Way.

Both of the above methods are basically sound. But, the results obtained from the second method are more reliable. The range of error for the samples measured by method B, range from a low of approximately two-percent (2%) to a maximum of twenty-five percent (25%). For method A, the range of error was estimated between 5% and 25%. This range of error is inversely related to the sample size. The smaller the sample the greater the probable error.

2. Impregnation of Basalt with Plastic Monomer.

After the determination of bulk vesicularity, the samples were impregnated with a polystyrene monomer. This monomer consisted of a polyester resin solution thinned with a styrene monomer. The polystyrene monomer was a mixture of these two, and was in the following proportions: Polyester resin solution-80% and styrene monomer 20%. The addition of the styrene monomer was necessary to reduce the polyester resins' viscosity to sightly more than water. Further, a catalyst (methyl-ethyl keytone peroxide) was added to this mixture to facilitate hardening of the plastic. It was determined that only 1ml of catalyst was needed to adequately polymerized the plastic. Use of excess catalyst resulted in cracking of the plastic during curing.

Polystyrene monomer was mixed in a 500ml plastic beaker and placed into a bell jar. A platform was constructed within the bell jar to hold the sample above the polystyrene monomer. The bell jar was evacuated, with a constant vacuum held for two minutes. The bell jar was tipped from vertical, just enough to cause the sample to fall into the polystyrene monomer. The vacuum was continued for another 2 minutes with air allowed to re-enter the bell jar slowly after 2 minutes The return to 1 bar caused the polystyrene monomer to impregnate the sample.

Evidently, there is a very open network of pores within basalts, since it was observed that all vesicles were filled with plastic as the samples were cut for dissolution.

The impregnated samples were placed in an oven at 70°C for three days. (The oven was placed inside a fume hood, because the odor of polystyrene monomer is quite powerful and can be a health threat if sufficient quantity is inhaled.) The samples were removed from the oven and allowed to cool for several more days.

Samples were removed from the plastic beakers by inverting the beaker and tapping the beakers' "top" firmly on a hard surface. Excess plastic was cut from the samples using a diamond-paste rock saw. The cuts were made to remove the minimum amount of sample as possible. Generally, less than 1.5mm of material was removed from each side of the sample proper. After the excess was removed, the samples were marked for identification and were thus ready for dissolution in HF.

It was determined about half-way through the experiment that smaller samples were required due to the large number of the bubbles encountered in samples 1-15. For example, sample number 6 was determined to contain a total of 11864 bubbles and took nearly 35 hours to count. Obviously, statistics do not require that such a vast number of bubbles be counted, so samples 16-29 were processed differently that the first set of samples.

The remaining samples were cut to about 3/4 the size of the first batch of samples, that is, they contained 25% less volume than sets 1-15. They were impregnated with polystyrene monomer as the other samples were, and the excess plastic was removed in the same way. However, depending on the size of the sample impregnated, the sample was cut in half longitudinally with only one-half of the sample being dissolved. The remaining sample was kept and labeled for possible future investigations. This change in procedure resulted in fewer bubbles to count, but still within statistically acceptable standards with the

smallest bubble count being 403, in sample 21R

3. Dissolution of the Basalt to recover the casts (bubbles).

The basalt is dissolved with 49% Hydrofluoric acid (HF). This acid is especially dangerous since it is odorless, tasteless, and colorless. 4ppm is considered the threshold for an IDLH (Immediately Dangerous to Life or Health) situation. All work involving HF was performed in a hood certified for its use. All metal and glass surfaces inside the hood were coated with a plastic film (like that available to seal Polaroid instant pictures) before work was begun. HF reacts with most metals including stainless steel. It is recommended that investigators consult their respective Environmental Health and Safety office for further HF handling guidelines.

The samples were placed within 6-household plastic 2-qt. pitchers with strainer tops. The containers were marked with the sample number and date. HF was decanted into these containers. Approximately 500ml was poured into each container, or enough to cover the sample by at least 0.5cm.

The containers were placed inside a large plastic tub that was 1/3 filled with slaked lime (hydrated lime, CaOH). This prevents HF from escaping unneutralized if a container is upset, or if HF solution is dropped. The tub was placed on rubber stoppers to elevate it from the fume hood "floor." Allowing for a free flow of air under and around the containers.

Dissolution time varied and depended on initial sample size. Large samples took up to 4 weeks to dissolve, smaller ones as little as 2 weeks. When the basalt had completely dissolved, the solution was neutralized. For each batch of 3, 2-quart containers, 3, 400ml beakers filled with slaked lime were placed in a plastic gallon container. Water was added slowly to the slaked lime and was stirred by a commercial paint stirrer attached to a power drill. Water was added until the solution was similar in viscosity to 5W-30 motor oil. The solution was strained

through a sieve, with 0.40mm openings, into another plastic, gallon container, removing many insoluble granules that would make later counting of the vesicle casts more difficult. Approximately 1 quart of cold water was added to the HF containing containers. The slaked lime solution was poured SLOWLY into the HF solution. The reaction was (is) exothermic, which was (is) cause for caution. The boiling point for HF is approximately 55°C and temperatures observed during the neutralization process were as high as 80°C. This resulted in a HF vapor being evolved from the solution. The HF vapor was minimized when large amounts of cold water were present at the start of neutralization.

The slaked lime solution was added until the pH of the resultant solution was between 5 and 9. At this point it was safe to handle in a hood. However, the solution was always allowed to cool to room temperature before attempting the removal of the plastic casts. This minimized the possibility of breathing HF vapor that might still be evolving due to the reaction.

After the solution had cooled, the mixture was stirred with the same paint stirrer as mentioned above and poured through a sieve with 0.75mm openings into another plastic, gallon container. The remaining mixture in the gallon container was then poured through a sieve of 0.45mm openings. Remaining waste solution was disposed of in accordance with applicable regulations.

The sieves now contained the vesicle casts that were segregated as indicated. The sieves and their contents were then washed with tap water to remove any additional impurities (ie, slaked lime granules not removed prior to this process). Casts were coaxed into a pile against the side of each sieve by the flow of water and were removed from the sieve and placed into their respective sample container marked with the sample size and number (ie, sample 6, size >0.5ø). These containers were placed into a hood to dry.

The HF containers were washed out and relabeled for the next batch of samples. The process was repeated until all samples were exhausted.

4. Counting the vesicle casts (bubbles).

After the casts dried, they were ready for counting. Counting entailed the division of casts into various size categories. These categories were: <0.75mm, 1mm, 2mm, 3mm, 4mm, 5mm, 6mm, 7mm, 8mm, 9mm, and 10mm (these are cast diameters). The casts were sized as if they were ideal spheres (Sahagian et al 1989) and coalesced casts were counted as separate casts only if their outline was clearly visible, that is, if less than 25% of their surface area was in contact with another sphere. If this was not the case, the coalesced casts' volumes were estimated as if they were a single sphere (Sahagian et al, 1989).

The estimation of cast size (diameter) and segregation of the casts, was facilitated by the use of 1mm grid graph paper. A 6x microscope enabled faster and more accurate counts. A lab point-counter was obtained to tabulate category counts.

Separate counts were made of the casts obtained from the samples derived by the 0.75mm sieve. These samples used the 0.75 through 10mm classification scheme. Casts derived from the 0.45mm sieve were not individually counted, but were estimated in total volume only. That is, what sized sphere would they make if they could be fused together.

This last procedure was added late into the experiment after it was noted these small casts really existed, therefore, only samples 19-29 have these data available. It was assumed there was little or no vesicle formation in the size range 0.45mm–0.75mm (personal communications with D. Sahagian). However, in some samples their contribution to bulk vesicularity can be significant.

After counting, the results were logged as total casts for each size (diameter) category. These numbers were used for calculation of vesicle size distribution as related to their volume fraction. Results are in appendix B in the form of tables and graphs.

Possible procedural error sources.

The plastic used in this experiment was quite resistant to the effects of HF. Saw marks made on the plastic casts remained sharp and defined for all samples. Further, right angle cuts through casts also remained sharp. This indicates that HF did not dissolve the plastic since sharp edges would become rounded due to their larger exposed surface area.

However, the classification of cast diameter (bubbles) was somewhat problematic. The problem was more apparent in the division between 1mm to 2mm than between other sizes. Many casts fell in-between 1 and 2mm and judgment calls were made as to where to put them. This judgment call was based on the fact that to be a 2mm cast it had to be at least 8 times greater in volume than an ideal 1mm cast. But, the assignment to 2mm class started at about 5-6 times the volume of a ideal 1mm cast. This resulted in overlapping of cast size classifications. Further, it was possible that, as many, or more, questionable 1mm casts were assigned to 2mm status, than questionable 2mm casts were assigned to 1mm status. But, overall 2mm casts represent the greatest volume percentage total, hence effects on calculated distributions should be minimal.

Observations.

Theoretically, larger bubbles within the melt should not entrain bubbles significantly smaller, because the larger velocity of the large bubbles would prevent the much smaller-bubble from coalescence. However, in several samples, bubbles 3 to 4mm in diameter have clearly entrained much smaller bubbles. These significantly smaller, entrained bubbles are usually less than 0.5mm in size. This was not expected. Bubbles of vastly different size should never touch. Small bubbles, having a lower velocity than larger bubbles, should be swept around the perimeter of the larger bubble in the fluid escape flow. Perhaps,these

bubbles were the result of wake capture (however, wake capture is not permitted in the model) (Sahagian et al, 1989).

The meaning of this observation in not immediately clear, however, it does show that this kind of coalescence can, and does occur. However, its frequency has not been quantified and its effect may be small.

Samples 1-14 have unimodal distributions. The mode is usually centered around 2-2.5mm. However, the volume percentage graphs change markably for samples 15-29, with most graphs strongly bi-modal, or even tri-modal. This is expected. Samples 1-14 were collected at low elevations (<1100ft.), while samples 15-29 were collected at high elevations (>12,900ft.). If atmospheric pressure can affect bubble (vesicle) size then its presence (sea-level) or absence (12,000ft.) should leave a signature in the basalt. Greater atmospheric pressure should cause more, smaller diameter vesicles. Whereas, lesser amounts of atmospheric pressure should cause more, larger vesicles. If the numerical model is to be proved valid, the model needs to predict larger bubbles at higher elevations. Indeed, this is the case. The model strongly correlates with the observed results.

Results.

The results of the experiment are given graphically in Figures 2 through 7. They indicate that a strong correlation exists between the model, vesicle (bubble) size distribution, and the observed distribution from natural basalts.

Flows from locality 1 (at 150' elevation above sea level), and locality 7 (at 12,900' elevation above sea level) show differences in vesicle (bubble) size distribution between top and bottom of the flows. The difference between top and bottom is greater for locality 7 at the Mauna Loa summit, as expected. Both the model and the laboratory results show this.

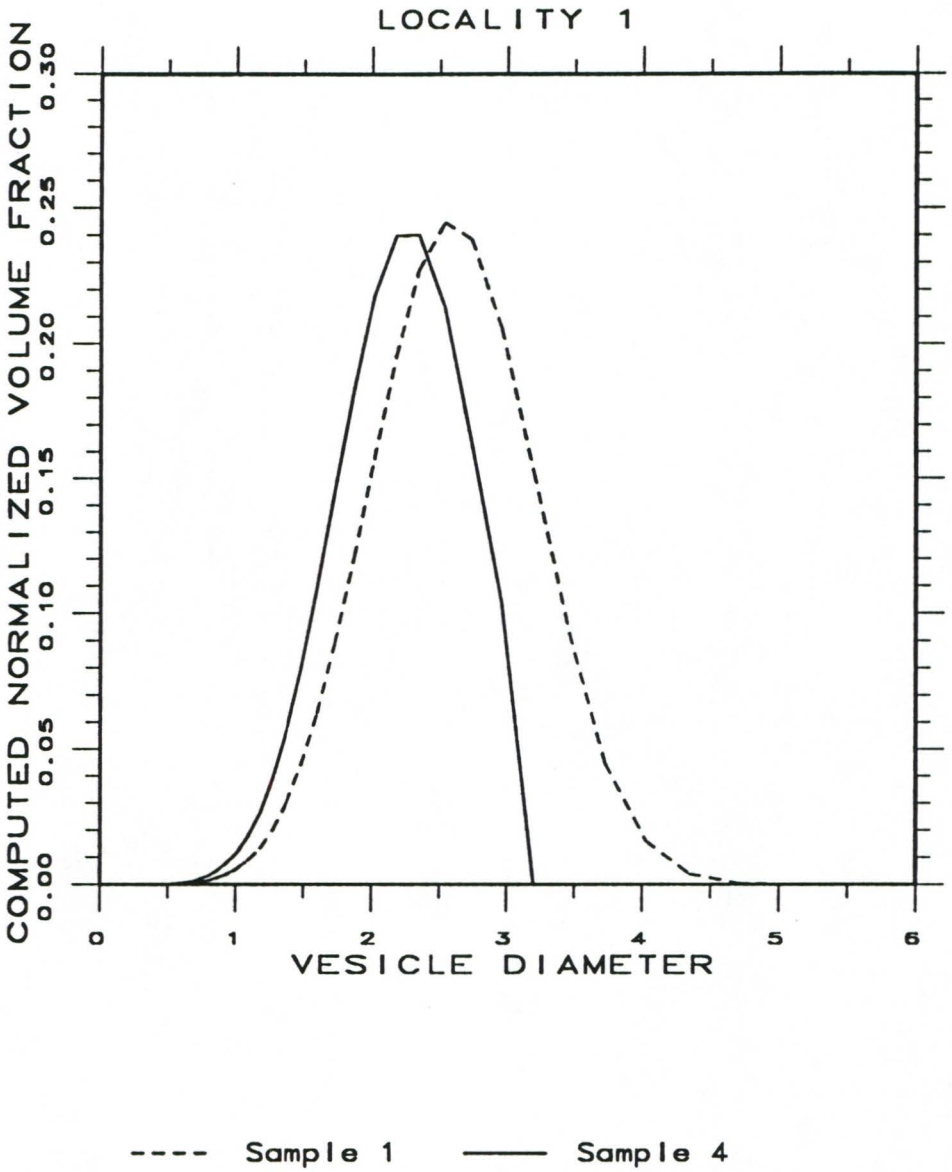

Figure 2. Graph of data from the model is as indicated. Laboratory data is omitted for clarity. As you might recall from table 1 in the text, Sample 1 is the top of the flow at locality 1 and sample 4 is the base of the same flow. See figures 3 and 4 for the plot of laboratory data with computed data.

In this study, data derived from the model is used to compute the atmospheric pressure, in this case the result is 0.96 bar, which closly matches the actual value of 1 bar.

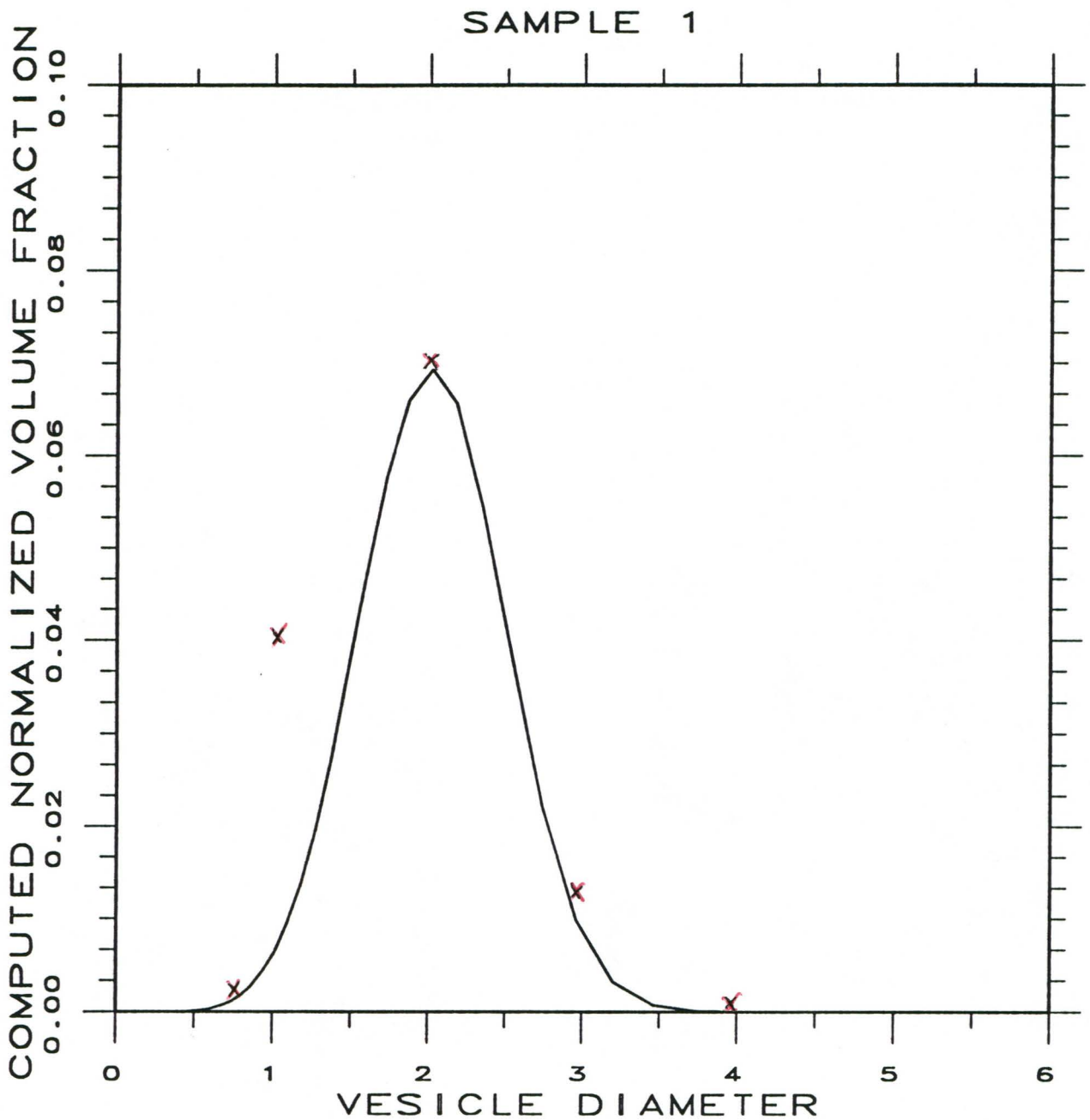

Figure 3. Graph of data from the model is as indicated. Laboratory data is given by the red "x's" and has been normalized to the computed axis.

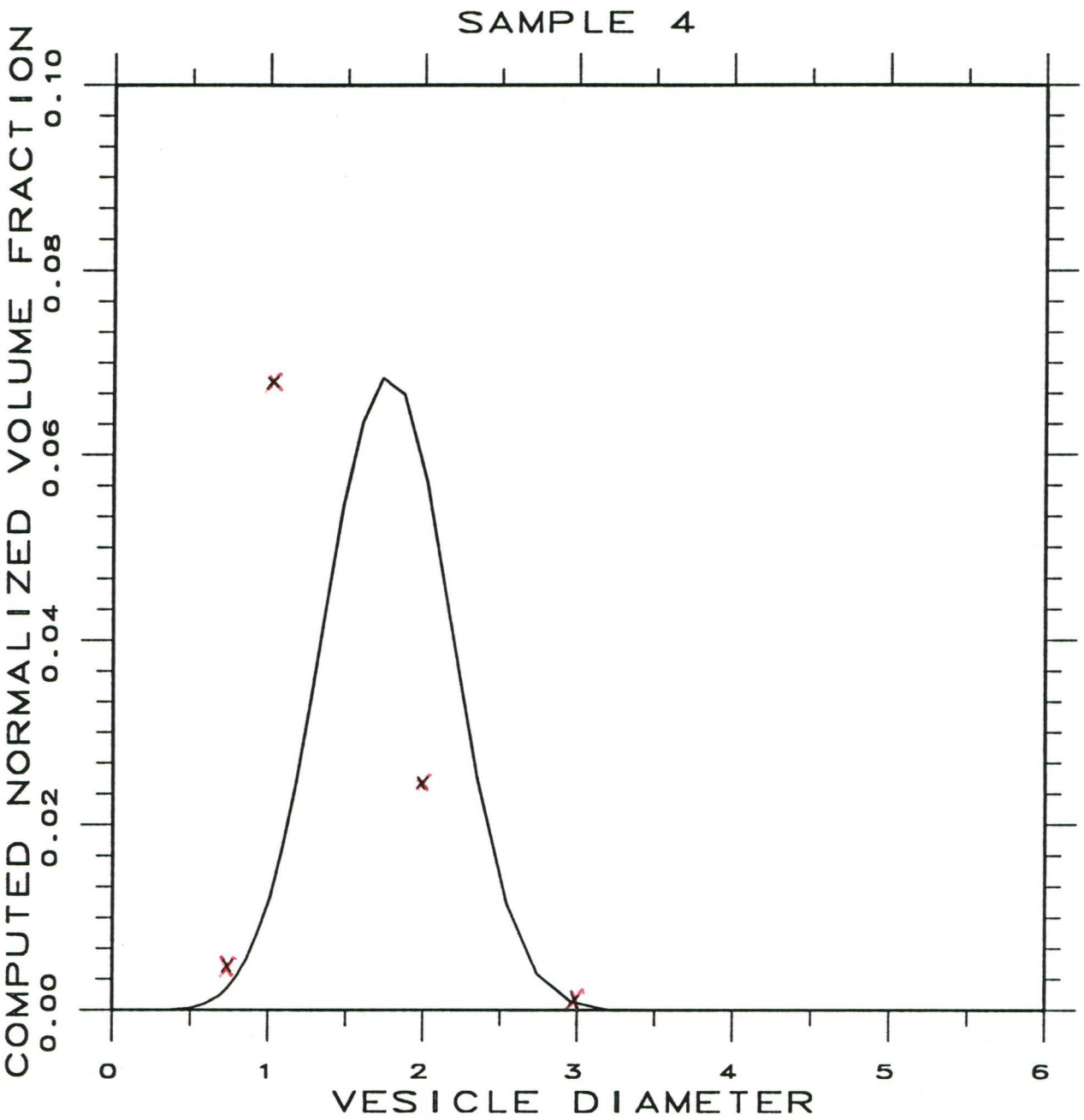

Figure 4. Graph of data from the model is as indicated. Laboratory data is given by the red "x's" and has been normalized to the computed axis.

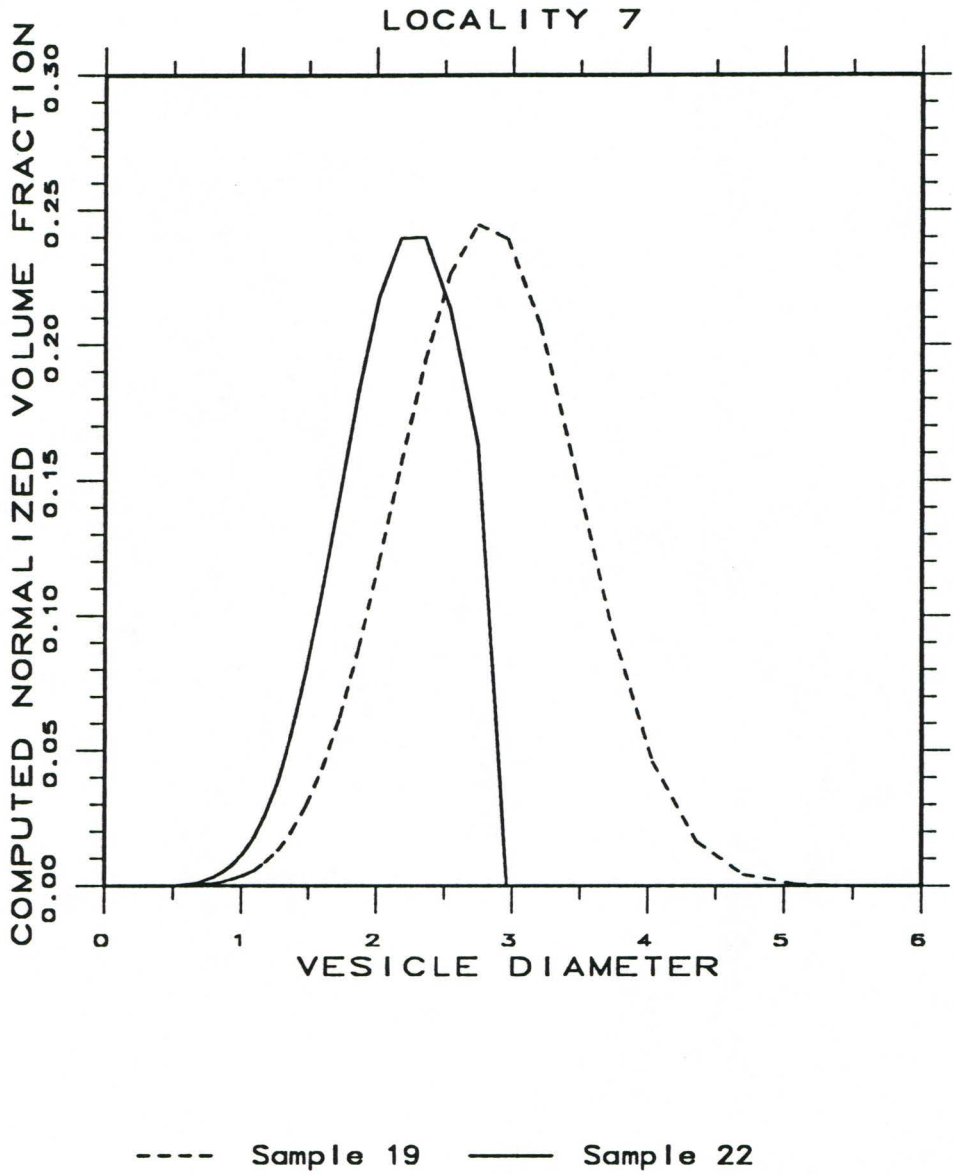

Figure 5. Graph of data from the model is as indicated. Laboratory data is omitted for clarity. As you might recall from table 1 in the text, Sample 19 is the top of the flow at locality 7and sample 22 is the base of the same flow. See figures 6 and 7 for the plot of laboratory data with computed data.

In this study, data derived from the model is used to compute the atmospheric pressure, in this case the result is 0.46 bar, which closly matches the actual value of 0.6 bar.

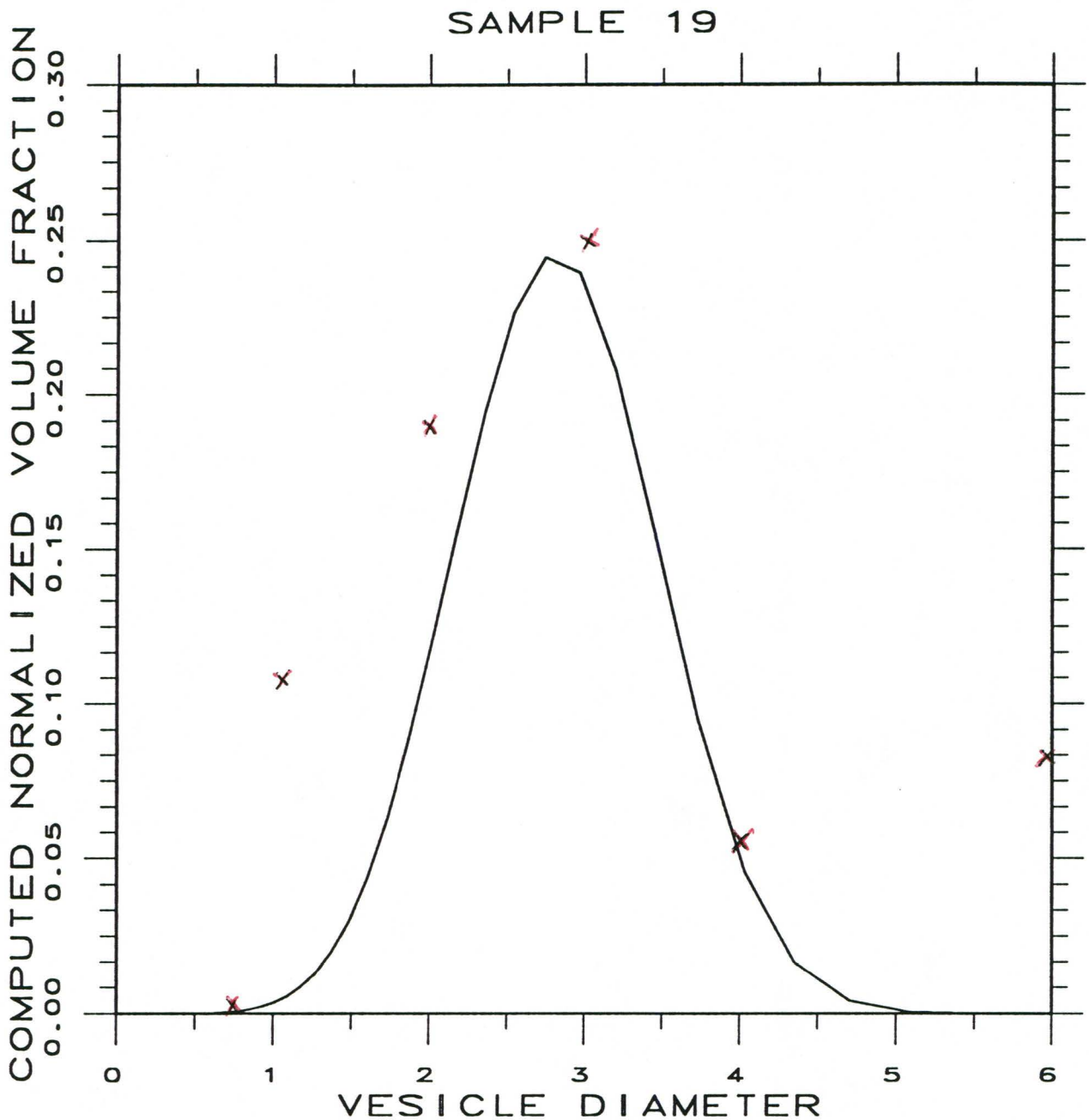

Figure 6. Graph of data from the model is as indicated. Laboratory data is given by the red "x's" and has been normalized to the computed axis.

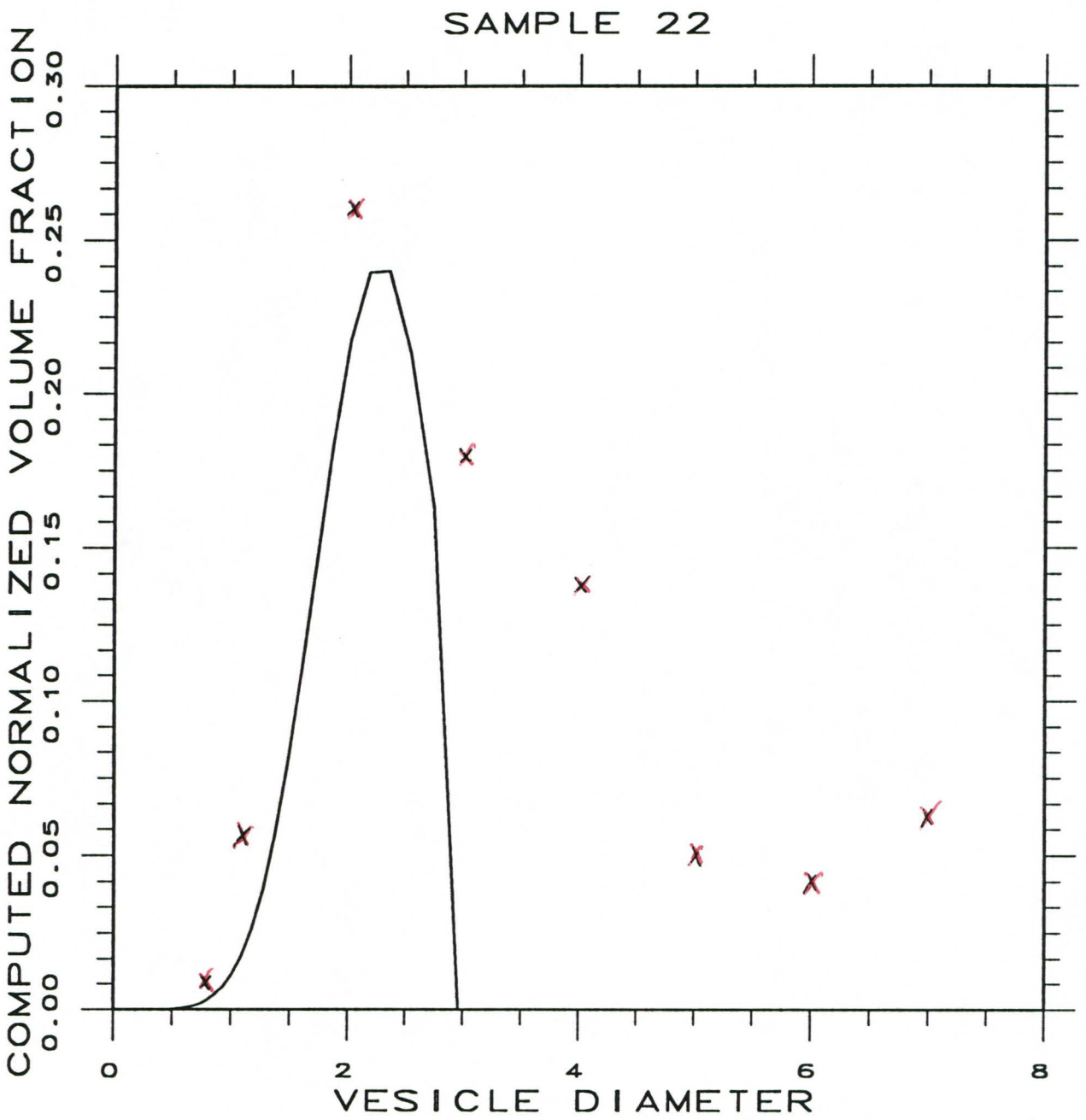

Figure 7. Graph of data from the model is as indicated. Laboratory data is given by the red "x's" and has been normalized to the computed axis.

Thus, atmospheric pressure can be calculated from the following simple relation:

$$\frac{V_t}{V_b} = \frac{\{\rho g H + P\}}{P} \qquad (2)$$

Where V_t and V_b are the vesicularities at the top and the bottom of the flow, respectively, lava density is ρ, g is the gravitational constant, and H is flow thickness. P is atmospheric pressure at the time and altitude of emplacement (Sahagian et al, 1989).

The results of the calculations (data are from the model) for locality 1 and 7 are: 0.96 bar and 0.46 bar respectively. The calculated results closely match the actual values of 1 bar and 0.6 bar respectively.

This correlation validates the model. We can now use this technique to determine paleobarometric measurements if elevation of basalt emplacement is known, or conversely, the technique can be used to determine the paleoelevation if paleopressures are assumed.

Conclusions.

The actual observed basalt flow characteristics correlate strongly with those predicted by the numerical model. Therefore, the model is valid for flows of this type. Indeed, atmospheric pressure can be measured directly from the ratio of vesicle (bubble) size distributions, from either the model (given flow parameters) or empiric data.

However, atmospheric pressure depends on elevation, so by using this technique one can determine paleoelevation and hence, construct the paleogeography. Further, atmospheric pressure may have varied with geologic time. If suitable flows can be constrained, in regards to elevation of

emplacement, paleopressures of the fossil atmosphere can be determined. Giving investigators new, possibly profound insights into the Earth's atmospheric evolution. In addition, this technique is not limited in application to the Earth, but rather, it can be applied to atmospheres of other terrestrial planets within the solar system, with the effect of providing insight into their atmospheric evolution as well.

Acknowledgments.–The author is thankful to Ashland Chemical, Inc. which provided the polyester resin solution and Dow Chemical, Inc., which provided the styrene monomer. Also, thanks to Dr. Sahagian for his help and guidance throughout this research, Michelle Jones who helped with the pulling of reference materials, and (now) Sara Maus, who put up with the late nights while the research was in progress.

References cited:

Gerlach, T., 1986, Exsolution of H_2O, CO_2, and S during eruptive episodes of Kilauea volcano, Hawaii: Journal of Geophysical Research, vol. 91, p. 12,177-12,185.

Mangan, M. T., Cashman, K. V., and Newman, S., 1993, Vesiculation of basaltic magma during eruption: Geology, vol. 21, p. 157-160.

Sahagian, D. L., 1985, Bubble migration and coalescence during the solidification of basaltic lava flows: Journal of Geology, vol. 93, p. 205-211.

Sahagian, D. L., Anderson, A. T., and Ward, B., 1989, Bubble coalescence in basalt flows: comparisons of a numerical model with natural examples: Bulletin of Volcanology, vol. 52, p. 49-56.

Shafer, N. E., and Zare, R. N., 1991, Through a beer glass darkly: Physics Today, Oct. 1991, p. 48-52.

Sparks, R. S. J., 1978, The dynamics of bubble formation and growth in magmas: a review and analysis: Journal of Volcanology and Geothermal Research, vol. 3, p. 1-37.

Spera, F., Yuen, D., and Kirschvink, S., 1982, Thermal boundary layer convection in silicic magma chambers: effects of temperature-dependent rheology and implications for thermogravitational chemical fractionation: Journal of Geophysical Research, vol. 87, p. 8755-8767.

The Times atlas of the world, 1985, Hawaii, 1:1,000,000 series, plate 114.

USGS base map, 1975, Hawaii, 1:250,000 series.

Appendix A: Results of bulk vesicularity determination.

Volume Measurements for bulk vesicularity determination, Method "A."

Sample Number	Mass in air (Ma) (in grams)	Mass in water (Mw) (in grams)	vol. rock= Ma-Mw	Rock Density	Bulk Vesicularity
1	845.22	410.00	435.2	1.94	0.35
2	427.70	170.00	257.7	1.66	0.44
3	187.60	86.90	100.7	1.86	0.37
4	144.05	56.00	88.1	1.63	0.45
5	454.70	121.00	333.7	1.36	0.54
6	654.10	82.00	572.1	1.14	0.61
7	57.80	16.00	41.8	1.38	0.53
8	155.80	57.90	97.9	1.59	0.47
9	421.50	135.50	286.0	1.47	0.50
10	520.60	80.00	440.6	1.17	0.60
11	198.00	43.60	154.4	1.28	0.57
12	559.45	180.10	379.4	1.47	0.50
13	285.80	118.00	167.8	1.70	0.43
14	54.10	14.00	40.1	1.34	0.55
15	125.40	48.50	76.9	1.63	0.45
16	520.50	218.30	302.2	1.72	0.42
17	833.60	392.50	441.1	1.79	0.40
18	690.10	288.00	402.1	1.71	0.42
19	433.40	198.00	235.4	1.85	0.38
20	896.15	437.50	458.7	1.95	0.34
21	1335.20	488.50	846.7	1.57	0.47
22	1389.10	643.50	745.6	1.86	0.37
23	247.40	93.50	153.9	1.60	0.46
24	521.00	238.50	282.5	1.84	0.38
25	245.90	71.30	174.6	1.40	0.53
26	18.15	7.50	10.7	1.70	0.43
27	434.00	214.40	219.6	1.97	0.34
28	1145.35	1145.35	0.0	0.00	0.00
29	53.90	27.60	26.3	2.04	0.31

Volume Measurements for bulk vesicularity determination, Method "B."

Sample Number	Water Volume (to begin with)	Water Volume with sample after 5min. vacuum	Net volume with pores filled with water	Water Volume with sample encased with tape and wax (100ml start)	weight of encasement materials (in grams)	Correction Factor see below (density) g/ml	Volume of bubbles	Bulk Vesicularity
1	110	142.0	32.0	152.0	5.500	1	14.50	0.31
2	100	124.0	24.0	150.0	4.560	0.911	20.99	0.47
3	100	117.0	17.0	132.5	2.940	0.911	12.27	0.42
4	100	114.0	14.0	127.0	3.460	0.911	9.20	0.40
5	100	120.0	20.0	146.0	3.975	0.911	21.64	0.52
6	75	89.5	14.5	144.0	3.765	0.911	25.37	0.64
7	50	58.0	8.0	110.0	1.589	0.868	0.17	0.02
8	85	100.0	15.0	131.0	3.420	0.911	12.25	0.45
9	80	92.0	12.0	129.0	3.420	0.911	13.25	0.52
10	100	122.0	22.0	142.0	4.250	0.911	15.33	0.41
11	100	116.0	16.0	139.0	2.880	0.911	19.84	0.55
12	n/a	n/a	n/a	n/a	n/a	n/a	n/a	n/a
13	100	120.0	20.0	135.0	2.850	0.911	11.87	0.37
14	n/a	n/a	n/a	n/a	n/a	n/a	n/a	n/a
15	75	85.0	10.0	120.0	2.120	0.911	7.67	0.43
16	90	122.0	32.0	152.5	3.380	0.911	16.79	0.34
17	85	106.0	21.0	140.0	5.950	0.868	12.15	0.37
18	85	98.0	13.0	125.0	2.220	0.911	9.56	0.42
19l	85	103.0	18.0	130.0	2.490	0.911	9.27	0.34
20l	80	97.0	17.0	128.0	2.700	0.911	8.04	0.32
21l	100	121.0	21.0	143.0	3.760	0.911	17.87	0.46
22r	100	127.0	27.0	145.0	3.630	0.911	14.02	0.34
23l	85	98.0	13.0	129.0	2.970	0.911	12.74	0.49
24l	85	107.0	22.0	136.5	2.497	0.911	11.76	0.35
25r	80	94.0	14.0	130.5	2.475	0.911	13.78	0.50
26a	60	64.5	4.5	113.0	3.450	0.868	4.53	0.50
26b	50	52.0	2.0	110.0	1.910	0.868	5.80	0.74
27r	90	112.0	22.0	135.5	4.610	0.868	8.19	0.27
28t	90	109.5	19.5	138.5	2.957	0.911	15.75	0.45
29	80	99.0	19.0	126.0	3.367	0.868	3.12	0.14

Notes: Wax was determined to be 4.425g/5ml which equals 0.885 g/ml
Masking tape was determined to be 0.469g/0.5ml which equals 0.938g/ml
The average of these two densities together is 0.911g/ml, which is used for the correction factor
Due to missing tape: different values are obtained by
new tapes density at 0.85g/ml, this leads to new average of 0.868g/ml.

Appendix B: Results of laboratory analysis of natural basalt samples.

This is the data for volume fraction compared with vesicle radius.
rev 3, 8-19-93

NOTE: % vol. fraction has been normalized in the following calculations.

Sample Number	>0.75 m	1mm	2mm	3mm	4mm	5mm	6mm	7mm	8mm	9mm	10mm	11mm	12mm	Total no. of Vesicles	Total Vol. of vesicles
1	1805	11167	2394	139	6									15511	
	399	5847	10028	1965	201	0	0	0	0	0	0	0	0		18440
	0.75	1.00	2.00	3.00	4.00	5.00	6.00	7.00	8.00	9.00	10.00	11.00	12.00		
% vol. fraction	0.02	0.32	0.54	0.11	0.01	0.00	0.00	0.00	0.00	0.00	0.00	0.00	0.00		
2	0	223	362	260	70	9	3							927	
	0	117	1516	3676	2346	589	339	0	0	0	0	0	0		8583
	0.75	1	2	3	4	5	6	7	8	9	10	11	12		
% vol. fraction	0.00	0.01	0.18	0.43	0.27	0.07	0.04	0.00	0.00	0.00	0.00	0.00	0.00		
3		338	358	123	13	1								833	
	0	177	1500	1739	436	65	0	0	0	0	0	0	0		3917
	0.75	1.00	2.00	3.00	4.00	5.00	6.00	7.00	8.00	9.00	10.00	11.00	12.00		
% vol. fraction	0.00	0.05	0.38	0.44	0.11	0.02	0.00	0.00	0.00	0.00	0.00	0.00	0.00		
4	944	6409	278	5	2									7638	
	209	3356	1164	71	67	0	0	0	0	0	0	0	0		4866
	0.75	1.00	2.00	3.00	4.00	5.00	6.00	7.00	8.00	9.00	10.00	11.00	12.00		
% vol. fraction	0.04	0.69	0.24	0.01	0.01	0.00	0.00	0.00	0.00	0.00	0.00	0.00	0.00		
5	433	1191	208	14	1									1847	
	96	624	871	198	34	0	0	0	0	0	0	0	0		1822
	0.75	1.00	2.00	3.00	4.00	5.00	6.00	7.00	8.00	9.00	10.00	11.00	12.00		
% vol. fraction	0.05	0.34	0.48	0.11	0.02	0.00	0.00	0.00	0.00	0.00	0.00	0.00	0.00		

6	89	7337	4310	122	6									11864	
	20	3842	18054	1725	201	0	0	0	0	0	0	0	0		23841
	0.75	1.00	2.00	3.00	4.00	5.00	6.00	7.00	8.00	9.00	10.00	11.00	12.00		
% vol. fraction	0.00	0.16	0.76	0.07	0.01	0.00	0.00	0.00	0.00	0.00	0.00	0.00	0.00		
7	7016	1307	34	2										8359	
	1550	684	142	28	0	0	0	0	0	0	0	0	0		2405
	0.75	1.00	2.00	3.00	4.00	5.00	6.00	7.00	8.00	9.00	10.00	11.00	12.00		
% vol. fraction	0.64	0.28	0.06	0.01	0.00	0.00	0.00	0.00	0.00	0.00	0.00	0.00	0.00		
8	313	609	93	12										1027	
	69	319	390	170	0	0	0	0	0	0	0	0	0		947
	0.75	1.00	2.00	3.00	4.00	5.00	6.00	7.00	8.00	9.00	10.00	11.00	12.00		
% vol. fraction	0.07	0.34	0.41	0.18	0.00	0.00	0.00	0.00	0.00	0.00	0.00	0.00	0.00		
9		868	992	462	106	13	2	2	1					2446	
	0	454	4155	6531	3552	851	226	359	268	0	0	0	0		16398
	0.75	1.00	2.00	3.00	4.00	5.00	6.00	7.00	8.00	9.00	10.00	11.00	12.00		
% vol. fraction	0.00	0.03	0.25	0.40	0.22	0.05	0.01	0.02	0.02	0.00	0.00	0.00	0.00		
10	273	422	99	13										807	
	60	221	415	184	0	0	0	0	0	0	0	0	0		880
	0.75	1.00	2.00	3.00	4.00	5.00	6.00	7.00	8.00	9.00	10.00	11.00	12.00		
% vol. fraction	0.07	0.25	0.47	0.21	0.00	0.00	0.00	0.00	0.00	0.00	0.00	0.00	0.00		
11	316	198	95	8	1	1								619	
	70	104	398	113	34	65	0	0	0	0	0	0	0		783
	0.75	1.00	2.00	3.00	4.00	5.00	6.00	7.00	8.00	9.00	10.00	11.00	12.00		
% vol. fraction	0.09	0.13	0.51	0.14	0.04	0.08	0.00	0.00	0.00	0.00	0.00	0.00	0.00		

12	Sample impregnated with soil and other organic debris.													0	
13	400	1013	183	34	5	2								1637	
	88	530	767	481	168	131	0	0	0	0	0	0	0		2164
	0.75	1.00	2.00	3.00	4.00	5.00	6.00	7.00	8.00	9.00	10.00	11.00	12.00		
% vol. fraction	0.04	0.25	0.35	0.22	0.08	0.06	0.00	0.00	0.00	0.00	0.00	0.00	0.00		
14		3087	1120	166	19	4								4396	
	0	1616	4691	2347	637	262	0	0	0	0	0	0	0		9553
	0.75	1.00	2.00	3.00	4.00	5.00	6.00	7.00	8.00	9.00	10.00	11.00	12.00		
% vol. fraction	0.00	0.17	0.49	0.25	0.07	0.03	0.00	0.00	0.00	0.00	0.00	0.00	0.00		
15	322	2954	707	90	5									4078	
	71	1547	2961	1272	168	0	0	0	0	0	0	0	0		6019
	0.75	1.00	2.00	3.00	4.00	5.00	6.00	7.00	8.00	9.00	10.00	11.00	12.00		
% vol. fraction	0.01	0.26	0.49	0.21	0.03	0.00	0.00	0.00	0.00	0.00	0.00	0.00	0.00		
16	42	343	132	73	17	6	3	2	0	1				619	
	9	180	553	1032	570	393	339	359	0	382	0	0	0		3816
	0.75	1.00	2.00	3.00	4.00	5.00	6.00	7.00	8.00	9.00	10.00	11.00	12.00		
% vol. fraction	0.00	0.05	0.14	0.27	0.15	0.10	0.09	0.09	0.00	0.10	0.00	0.00	0.00		
17	Cannot be determined, too vesicular													0	
															0
18	163	973	252	44	7	1								1440	
	36	509	1056	622	235	65	0	0	0	0	0	0	0		2523
	0.75	1.00	2.00	3.00	4.00	5.00	6.00	7.00	8.00	9.00	10.00	11.00	12.00		
% vol. fraction	0.01	0.20	0.42	0.25	0.09	0.03	0.00	0.00	0.00	0.00	0.00	0.00	0.00		

19L	28	452	90	38	11	2		1						622	
	6	237	377	537	369	131	0	180	0	0	0	0	0		1836
	0.75	1.00	2.00	3.00	4.00	5.00	6.00	7.00	8.00	9.00	10.00	11.00	12.00		
% vol. fraction	0.00	0.13	0.21	0.29	0.20	0.07	0.00	0.10	0.00	0.00	0.00	0.00	0.00		
20L	444	671	156	42	7	3	1							1324	
	98	351	653	594	235	196	113	0	0	0	0	0	0		2241
	0.75	1.00	2.00	3.00	4.00	5.00	6.00	7.00	8.00	9.00	10.00	11.00	12.00		
% vol. fraction	0.04	0.16	0.29	0.26	0.10	0.09	0.05	0.00	0.00	0.00	0.00	0.00	0.00		
21R	44	222	79	28	8	8	7	3	2	1	1			403	
	10	116	331	396	268	524	792	539	536	382	524	0	0		4416
	0.75	1.00	2.00	3.00	4.00	5.00	6.00	7.00	8.00	9.00	10.00	11.00	12.00		
% vol. fraction	0.00	0.03	0.07	0.09	0.06	0.12	0.18	0.12	0.12	0.09	0.12	0.00	0.00		
22R	469	568	337	70	20	4	2	2						1472	
	104	297	1412	990	670	262	226	359	0	0	0	0	0		4320
	0.75	1.00	2.00	3.00	4.00	5.00	6.00	7.00	8.00	9.00	10.00	11.00	12.00		
	0.02	0.07	0.33	0.23	0.16	0.06	0.05	0.08	0.00	0.00	0.00	0.00	0.00		
23L	56	634	227	48	4	3								972	
	12	332	951	679	134	196	0	0	0	0	0	0	0		2304
	0.75	1.00	2.00	3.00	4.00	5.00	6.00	7.00	8.00	9.00	10.00	11.00	12.00		
% vol. fraction	0.01	0.14	0.41	0.29	0.06	0.09	0.00	0.00	0.00	0.00	0.00	0.00	0.00		
24L	162	439	124	27	4	2								758	
	36	230	519	382	134	131	0	0	0	0	0	0	0		1432
	0.75	1.00	2.00	3.00	4.00	5.00	6.00	7.00	8.00	9.00	10.00	11.00	12.00		
% vol. fraction	0.02	0.16	0.36	0.27	0.09	0.09	0.00	0.00	0.00	0.00	0.00	0.00	0.00		

25L	481	1117	189	43	5	2		1						1838	
	106	585	792	608	168	131	0	180	0	0	0	0	0		2569
	0.75	1.00	2.00	3.00	4.00	5.00	6.00	7.00	8.00	9.00	10.00	11.00	12.00		
% vol. fraction	0.04	0.23	0.31	0.24	0.07	0.05	0.00	0.07	0.00	0.00	0.00	0.00	0.00		
26A	77	206	57	9	6									355	
	17	108	239	127	201	0	0	0	0	0	0	0	0		692
	0.75	1.00	2.00	3.00	4.00	5.00	6.00	7.00	8.00	9.00	10.00	11.00	12.00		
	0.02	0.16	0.35	0.18	0.29	0.00	0.00	0.00	0.00	0.00	0.00	0.00	0.00		
27R	253	745	152	19	6	1								1176	
	56	390	637	269	201	65	0	0	0	0	0	0	0		1618
	0.75	1.00	2.00	3.00	4.00	5.00	6.00	7.00	8.00	9.00	10.00	11.00	12.00		
% vol. fraction	0.03	0.24	0.39	0.17	0.12	0.04	0.00	0.00	0.00	0.00	0.00	0.00	0.00		
28L	1104	870	98	28	21	8	0	1	0	1				2131	
	244	456	411	396	704	524	0	180	0	382	0	0	0		3294
	0.75	1.00	2.00	3.00	4.00	5.00	6.00	7.00	8.00	9.00	10.00	11.00	12.00		
% vol. fraction	0.07	0.14	0.12	0.12	0.21	0.16	0.00	0.05	0.00	0.12	0.00	0.00	0.00		
29	565	625	60	6										1256	
	125	327	251	85	0	0	0	0	0	0	0	0	0		788
	0.75	1.00	2.00	3.00	4.00	5.00	6.00	7.00	8.00	9.00	10.00	11.00	12.00		
% vol. fraction	0.16	0.42	0.32	0.11	0.00	0.00	0.00	0.00	0.00	0.00	0.00	0.00	0.00		